DETECTING LAND COVER CHANGE BY EVALUATING THE INTERNAL COVARIANCE MATRIX OF THE EXTENDED KALMAN FILTER

[†‡]B.P. Salmon, [†‡]W. Kleynhans, [‡]F. van den Bergh, [†]J.C. Olivier, and [‡]K.J. Wessels

[†]Department of Electrical, Electronic and Computer Engineering, University of Pretoria, South Africa

[‡]Remote Sensing Research Unit, Meraka Institute, CSIR, Pretoria, South Africa
bsalmon@csir.co.za

[†]School of Engineering, University of Tasmania, Australia

ABSTRACT

In this paper, the internal operations of an Extended Kalman Filter is investigated to see if any useful information can be derived to detect land cover change in a MODIS time series. The Extended Kalman Filter expands its internal covariance if a significant change in reflectance value is observed, followed by adapting the state parameters to compensate for this change. The analysis shows a change detection accuracy above 90% can be attained when evaluating the elements within the internal covariance matrix to detect new human settlements, with a corresponding false alarm rate below 11%.

Index Terms— Change detection algorithms, Covariance matrix, Kalman Filter, Spatial information, Time series analysis

1. INTRODUCTION

Remote sensing satellite data provide researchers with an effective way to monitor and evaluate land cover changes. An operator making an image-to-image comparison is still a common method in most organizations when mapping land cover change, which is time consuming and resource intensive. Automated change detection reduces human interaction and enables large data sets to be potentially processed in a fraction of the time. Change detection methods have been used as alerts to an operator to highlight potential areas where change has occurred. Many change detection methods that have been developed, only operate on the differences between two images. The limitation with only using two images is that similar land cover types can appear significantly different at various times of the year [1]. The temporal frequency of the remote sensing data acquisitions should be high enough to ensure the ability to distinguish between change events and phenological cycles. The high temporal frequency of coarse spatial resolution imagery makes it very attractive for change detection [2].

The Extended Kalman Filter (EKF) has previously been shown as a feature extraction method to model a NDVI time series for a given pixel as a triply modulated cosine function to improve land cover separation [3]. The objective of this paper is to evaluate the internal covariance matrix within the EKF, and observe if changes in land cover induces a significant deviations within the filter.

The paper is organized as follows. Section 2 discusses the study area and data set. In section 3 we present the method, and section 4 present the experimental results. Section 5 presents the conclusions.

2. STUDY AREA AND DATA DESCRIPTION

The study area is located in the Gauteng province, South Africa. The province is the most urbanized in the country. Large areas of natural vegetation exist within the province, but is converted to human settlements due to active migration to the province. The study area corresponds to a total area of approximately 285.5 km^2, which comprises 240.5 km^2 (962 pixels) no change areas and 45 km^2 (180 pixels) change areas. The time series were validated with visual inspection of SPOT images to map areas of *change*, and *no change* during the study period.

The MODIS (MCD43A4, Collection V005) 500 meter, Nadir and Bidirectional Reflectance Distribution Function (BRDF) adjusted spectral reflectance product was used, as it significantly reduces the anisotropic scattering effects of surfaces under different illumination and observation conditions [4, 5]. The data set provides an image every 8 days derived from a 16 day MODIS surface reflectance composite period. For each pixel a time series was extracted for the first two spectral bands from the data set (tile H20V11) (year 2000–2009).

3. METHODOLOGY

Kleynhans *et al.* proposed a method of using an EKF to model a NDVI time series using a triply modulated cosine function [3]. Salmon *et al.* extended on this method by modelling each spectral band independently [6], which is expressed as

$$y_{k,b} = \mu_{k,b} + \alpha_{k,b}\cos(\omega k + \phi_{k,b}) + v_{k,b}. \qquad (1)$$

The variable $y_{k,b}$ denotes the observed value of the b-th spectral band's time series, $b \in \{1, 2\}$ at time k. The additive

noise sample is denoted by $v_{k,b}$ and is assumed to be normally distributed. The cosine function model was separately fitted on each of the spectral bands and is based on several different parameters; the frequency ω, which is the same over both spectral bands, the nonzero mean $\mu_{k,b}$, the amplitude $\alpha_{k,b}$ and the phase $\phi_{k,b}$. The frequency was set to $8/365$. A state vector is estimated by the EKF at each time increment k, and is denoted by

$$\mathbf{x}_{k,b} = [\,\mu_{k,b}\;\;\alpha_{k,b}\;\;\phi_{k,b}\,]^T. \tag{2}$$

For the present case, it was assumed that the state vector $\mathbf{x}_{k,b}$ does not change significantly through time; hence, the process model $\mathbf{f}$ is linear. The measurement model $\mathbf{h}$, however, contains the cosine term and, as such, is evaluated via the standard Jacobian formulation, thereby linearizing the non-linear measurement model around the current state vector. Both these models are possibly non-perfect, so the addition of process noise $\mathbf{w}_{k,b}$ and measurement noise $v_{k,b}$ is required [7]. The process noise covariance matrix $\mathcal{Q}_{k,b}$ and observation noise covariance matrix $\mathcal{R}_{k,b}$ was set using the criterion described in [6]. The linear dynamic model for the EKF is thus expressed as

$$\mathbf{x}_{k,b} = \mathbf{f}(\mathbf{x}_{(k-1),b}) + \mathbf{w}_{k,b}, \tag{3}$$

and

$$\hat{y}_{k,b} = \mathbf{h}(\mathbf{x}_{k,b}) + v_{k,b}. \tag{4}$$

State vectors are estimated over time k based on the observation data $y_{k,b}$ up to time k [7]. The EKF recursively adapts the state vector for each incoming observation vector by predicting and updating the vector. In the prediction step, the state vector $\mathbf{x}_{(k|k-1),b}$ and internal covariance matrix $\mathfrak{B}_{(k|k-1),b}$ is predicted. The predicted state vector's estimate is computed as

$$\hat{\mathbf{x}}_{(k|k-1),b} = \mathbf{f}\Big(\hat{\mathbf{x}}_{(k-1|k-1),b}\Big), \tag{5}$$

and the predicted internal covariance matrix $\mathfrak{B}_{(k|k-1),b}$ is computed as

$$\mathfrak{B}_{(k|k-1),b} = \mathcal{Q}_{(k-1),b} + \mathbf{F}\mathfrak{B}_{(k-1|k-1),k}\mathbf{F}^{\mathrm{T}}. \tag{6}$$

The matrix $\mathbf{F}$ is the local linearization of the non-linear transition function $\mathbf{f}$. In the updating step the posterior estimate of the state vector $\hat{\mathbf{x}}_{(k|k),b}$ is computed as

$$\hat{\mathbf{x}}_{(k|k),b} = \hat{\mathbf{x}}_{(k|k-1),b} + \mathfrak{K}_{k,b}\Big(\mathbf{x}_{k,b} - \mathbf{h}\Big(\mathbf{x}_{k,b}\Big)\Big), \tag{7}$$

using the optimal Kalman gain denoted by $\mathfrak{K}_{k,b}$ which is computed as

$$\mathfrak{K}_{k,b} = \mathfrak{B}_{(k|k-1),b}\mathbf{H}^{\mathrm{T}}\mathcal{S}^{-1}_{k,b}. \tag{8}$$

The matrix $\mathbf{H}$ is the local linearization of the non-linear measurement function $\mathbf{h}$. The matrix $\mathcal{S}_{k,b}$ denotes the innovation term which is computed as

$$\mathcal{S}_{k,b} = \mathbf{H}\mathfrak{B}_{(k|k-1),b}\mathbf{H}^{\mathrm{T}} + \mathcal{R}_{k,b}. \tag{9}$$

The posterior estimate of the covariance matrix $\mathfrak{B}_{(k|k),b}$ is computed as

$$\mathfrak{B}_{(k|k),b} = \mathfrak{B}_{(k|k-1),b} - \mathfrak{K}_{k,b}\mathcal{S}_{k,b}\mathfrak{K}^{\mathrm{T}}_{k,b}. \tag{10}$$

The internal covariance matrix $\mathfrak{B}_{(k|k),b}$ is evaluated to observe any significant deviations when the EKF is subjected to a form of land cover change. It should be noted that the phase parameter $\phi_{k,b}$ provided negligible information to improve land seperability and was not evaluated further. The internal covariance matrix $\mathfrak{B}_{(k|k),b}$ is thus formally defined as

$$\mathfrak{B}_{(k|k),b} = \begin{pmatrix} \mathfrak{B}_{\mu\mu,k,b} & \mathfrak{B}_{\mu\alpha,k,b} \\ \mathfrak{B}_{\alpha\mu,k,b} & \mathfrak{B}_{\alpha\alpha,k,b} \end{pmatrix}, \tag{11}$$

with

$$\begin{aligned} \mathfrak{B}_{\mu\mu,k,b} &= \mathbf{E}(\mu_{k,b} - \mathbf{E}(\mu_{k,b}))^2 \\ \mathfrak{B}_{\mu\alpha,k,b} &= \mathbf{E}((\mu_{k,b} - \mathbf{E}(\mu_{k,b}))(\alpha_{k,b} - \mathbf{E}(\alpha_{k,b})) \\ \mathfrak{B}_{\alpha\mu,k,b} &= \mathbf{E}((\alpha_{k,b} - \mathbf{E}(\alpha_{k,b}))(\mu_{k,b} - \mathbf{E}(\mu_{k,b})) \\ \mathfrak{B}_{\alpha\alpha,k,b} &= \mathbf{E}(\alpha_{k,b} - \mathbf{E}(\alpha_{k,b}))^2. \end{aligned} \tag{12}$$

A labelled data set was used to evaluate the internal covariance matrix, with the no change time series presented with superscript nc and change time series with superscript c. The evaluation of the internal covariance matrix in this paper was only done 1-dimensionally on the elements $\mathfrak{B}_{\mu\mu,k,b}$ and $\mathfrak{B}_{\alpha\alpha,k,b}$. The change metric termed the Covariance Change Metric (CCM) $\delta_{\mu,k,b}$ is defined for the mean parameter as

$$\delta_{\mu,k,b} = \mathfrak{B}_{\mu\mu,k,b} - \mathbf{E}(\mathfrak{B}^{nc}_{\mu\mu,k,b}), \tag{13}$$

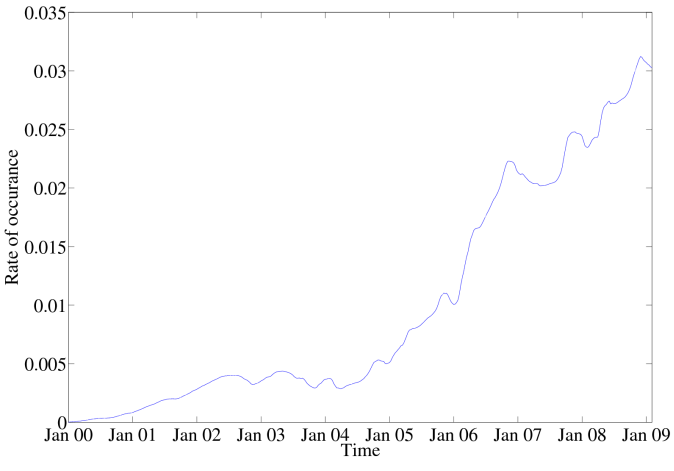

Fig. 1. A illustration of $\delta_{\mu,k,1}$ for an arbitrary pixel is given over the study period for the first MODIS spectral band.

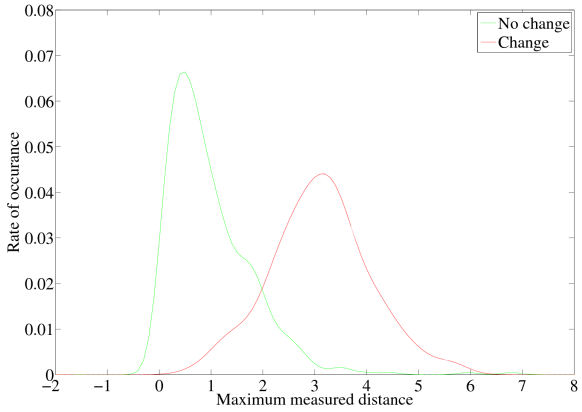

(a) Probability density functions computed for $\delta^{c}_{\mu,k,1}$ and $\delta^{nc}_{\mu,k,1}$ for the first MODIS spectral band.

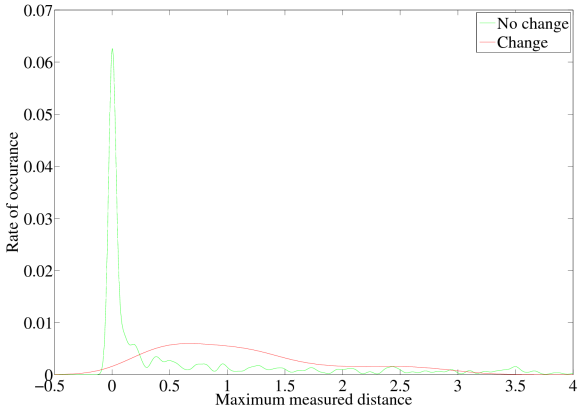

(b) Probability density functions computed for $\delta^{c}_{\mu,k,2}$ and $\delta^{nc}_{\mu,k,2}$ for the second MODIS spectral band.

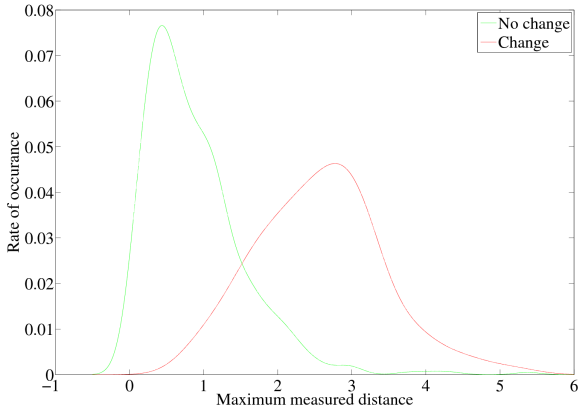

(c) Probability density functions computed for $\delta^{c}_{\alpha,k,1}$ and $\delta^{nc}_{\alpha,k,1}$ for the first MODIS spectral band.

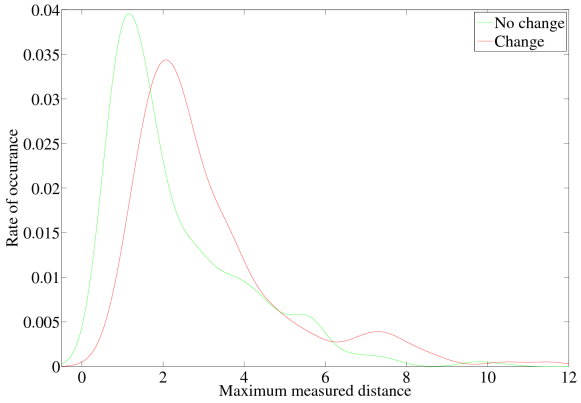

(d) Probability density functions computed for $\delta^{c}_{\alpha,k,2}$ and $\delta^{nc}_{\alpha,k,2}$ for the second MODIS spectral band.

Fig. 2. Comparisons on the separability between the change and no change probability density functions by evaluating different elements in the internal covariance matrix.

where $\mathfrak{B}_{\mu\mu,k,b}$ can be the element of an internal covariance matrix derived for a time series experiencing change or no change in land cover.

If the CCM $\delta_{\mu,k,b}$ of the mean parameter, exceeds a certain predefined threshold $\delta^{*}_{\mu,k,b}$, then the time series is flagged as an area that experienced land cover change. A similar CCM can be derived for the amplitude parameter and is denoted by $\delta_{\alpha,k,b}$.

4. RESULTS

4.1. Example of CCM

In this section an illustration is given on how the CCM changes over time when land cover change is present in the time series. In figure 1, the CCM is depicted for a single time series that has experienced land cover change within the study period. The CCM was computed using the changed time series as

$$\delta_{\mu,k,b} = \mathfrak{B}^{c}_{\mu\mu,k,b} - \mathbf{E}(\mathfrak{B}^{nc}_{\mu\mu,k,b}). \tag{14}$$

A significant change in the CCM $\delta_{\mu,k,1}$ in figure 1 started to emerge after January 2004. This signifies a change in land cover as the filter is adapting to a new stable state.

4.2. Change detection accuracies

In this section a Bayes' approach is used to investigate the change detection accuracies obtained in the study area. The land cover change of interest was the transformation of natural vegetation to newly formed human settlements. The behaviour of the diagonals in the internal covariance matrix were evaluated for the first two MODIS spectral bands. These probability distributions are shown in figure 2, where a clear separation between the change and no change time series is observed. The corresponding change detection accuracies (true positives) for the distributions shown in figure 2 are

reported in table 1, along with the correponding false alarms (false positive) in parentheses.

Table 1. Change detection accuracy measured on the labelled data set. Each entry gives the true positive accuracy with the corresponding false positive accuracy in parentheses.

	Metric	
	Mean parameter	Amplitude parameter
Spectral band 1	90.6% (10.5%)	90.0% (15.2%)
Spectral band 2	97.6% (39.8%)	82.1% (49.9%)

It is observed in table 1 that evaluating the internal covariance matrix to detect land cover change produces acceptable results when using the first MODIS spectral band. The second spectral band offered good change detection accuracies at the cost of high false alarms. The element $\mathfrak{B}_{\mu\mu,k,1}$ in the internal covariance matrix offers the best change detection accuracy.

Two well known methods have been implemented for comparison to the CCM. The first method is the annual NDVI differencing method by Lunetta *et al.* [1], which calculates the difference between consecutive summation of the annual NDVI time series. The pixel is flagged as change if a certain predefined threshold is exceeded in this difference. The threshold is usually determined using normal distribution statistics. The method reported change detection accuracy of 57% and a false alarm rate of 14% on the same data set.

The second method is the EKF change detection method by Kleynhans *et al.* [8], which evaluates the Euclidean distance between parameters derived with an EKF within a spatio-temporal window. The EKF fits a triply modulated cosine function to a time series to model the seasonal variations. The pixel is flagged as change if the Euclidean distance exceeds a predefined threshold. The method reported change detection accuracy of 75% and a false alarm rate of 13% on the same data set. In this case the CCM algorithm performed better than both these alternative change detection methods.

5. CONCLUSIONS

Previous research has shown that land cover change could be detected using the state parameters, which were estimated with an EKF [3, 6]. Good separation was obtained between the two classes when evaluating the mean and amplitude parameter that were estimated using the EKF. The EKF first alters the internal covariance matrix if a significant change in observation is observed, follow by adapting the state parameters. In this paper it was shown that information in the change of the internal covariance matrix can be used as change detection metric. The analysis showed change detection accuracies of +90% when using the first spectral band of MODIS with false alarms as low as 10.5%.

6. REFERENCES

[1] R.S. Lunetta, J.F. Knight, J. Ediriwickrema, J.G. Lyon, and L.D. Worthy, "Land-cover change detection using multi-temporal MODIS NDVI data," *Remote Sensing of Environment*, vol. 105, no. 2, pp. 142–154, November 2006.

[2] J. Borak, E. Lambin, and A. Strahler, "The use of temporal metrics for land cover change detection at coarse spatial scales," *International Journal of Remote Sensing*, vol. 21, no. 6, pp. 1415–1432, April 2000.

[3] W. Kleynhans et al., "Improving land cover class separation using an Extended Kalman Filter on MODIS NDVI Time-Series Data," *IEEE Geoscience and Remote Sensing Letters*, vol. 7, no. 2, pp. 381–385, April 2010.

[4] C. Schaaf et al., "First operational BRDF, albedo nadir reflectance product from MODIS," *Remote Sensing of Environment*, vol. 83, no. 1/2, pp. 135–148, November 2002.

[5] B.P. Salmon et al., "The use of a Multilayer Perceptron for detecting new human settlements from a time series of MODIS images," *International Journal of Applied Earth Observation and Geoinformation*, vol. 13, no. 6, pp. 873–883, December 2011.

[6] B.P. Salmon et al., "Meta-optimization of the Extended Kalman filter's parameters for improved feature extraction on hyper-temporal images," in *IEEE International Geoscience and Remote Sensing Symposium (IGARSS) 2011*, 2010, pp. 2543–2546.

[7] B. Ristic, S. Arulampalam, and N. Gordon, *Beyond the Kalman filter: Particle Filters for Tracking Applications*, Artech House, London, 1 edition, 2004.

[8] W. Kleynhans et al., "Detecting land cover change using an Extended Kalman Filter on MODIS NDVI time series data," *IEEE Geoscience and Remote Sensing Letters*, vol. 8, no. 3, pp. 507–511, May 2011.